CHEMISTRY OF MATERIALS

Article

pubs.acs.org/cm

Synthesis of Porous Metallic Monoliths via Chemical Reduction of Au(I) and Ag(I) Nanostructured Sheets

Gilles R. Bourret, Paul J. G. Goulet, and R. Bruce Lennox*

Department of Chemistry, McGill University, and Centre for Self-Assembled Chemical Structures (CSACS), 801 Sherbrooke Street West, Montréal, Québec H3A 2K6, Canada

Supporting Information

ABSTRACT: The facile fabrication of free-standing conductive Au(0) and Ag(0) nanostructured monoliths via the chemical reduction of sheets composed respectively of AuCl(*n*-butylamine) nanofibers and aggregated AgCl nanocubes is reported. This preparation can be performed on a large scale (hundreds of milligrams) with high yield (>74%). The product sheets have large dimensions (several cm^2), high conductivity (>1800 S m^{-1} for the Au(0) sheets), and large surface areas (2 m^2 g^{-1} or 400 m^2 mol^{-1} for the Au(0) sheets). The macroscopic structure of the Au(I) and Ag(I) sheets is preserved during the chemical reduction process. At the nanoscale the Au(I) fibers are converted into Au(0) ribbons and fibers, and the AgCl cubes are converted into porous Ag(0) cubes. The resulting porous metal sheets provide physically stable Au(0) and Ag(0) foams that are highly sought-after in catalysis, sensing, and electrocatalysis applications.

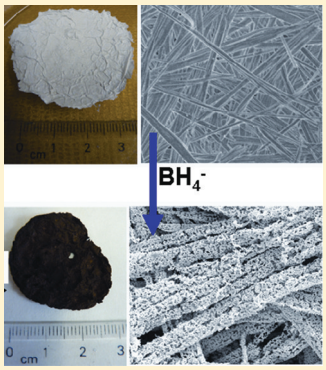

KEYWORDS: *gold, silver, porous, foam, monolith, sacrificial template*

INTRODUCTION

The properties and function of micro- and nanostructured materials often strongly depend upon their structure and morphology.[1] Catalysis, sensing, and photovoltaic activity are all greatly influenced by effective surface area. Porous materials are consequently much sought-after for these applications, and the synthesis of high surface area materials is an area of intense research.[1] Monolithic porous metals, usually referred to as foams or sponges, are particularly well-suited for these applications. They can be good conductors, have high surface areas, and typically demonstrate enhanced catalytic and plasmonic activity due to their nanoscale dimensions. Their monolithic nature enables their use in large scale processes while avoiding the need of a supporting substrate for many applications including those in batteries, hydrogen storage, SERS, antimicrobial materials, lightweight structures, and heat sinks, among others.[2]

The synthesis of a wide range of nonmetallic porous foams has been described, including metal oxides, metal chalcogenides, organic polymers, and carbon-based materials.[2] Despite their importance in electro- and heterogeneous catalysis, there are few reports concerning the controlled synthesis of porous metal monoliths. Classic processes for the fabrication of metallic foams include dealloying, template methods, sol–gel assembly of prefabricated nanoparticles, nanosmelting of hybrid polymer–metal oxide aerogels, and the combustion of metal complexes.[2] These methods, however, have intrinsic limitations including restriction to the fabrication of small monoliths, the requisite dissolution of the template or presynthesis of nanoparticles, restriction to metals that form stable oxides, or the use of high temperature and pressure, which can lead to impure materials.[2] These limitations can be avoided by producing porous metallic materials via the chemical reduction of solid assemblies of non-zero-valent nanostructures (NZVN, Figure 1). In this context, NZVN is a generic term used to describe stable nanoscale structures composed of either metal ionic crystals or coordination complexes. The designation NZVN is proposed in the context of their use as precursors in the formation of zerovalent metal nanostructures.

The use of solid species as precursors for metallic structure fabrication is, of course, well-established in black and white photography. In this case, the photoreduction of silver halides is the classic example of well-defined metallic nanostructures.[3,4] We recently reported the synthesis of well-defined linear assemblies of Au(0) nanoparticles with the thermolysis of Au(I) thiolate patterned via electron-beam lithography.[5] Qi et al. reported the chemical reduction of Ag_3PO_4 microcrystals into various Ag(0) structures.[6] These two early reports illustrate the versatility of using NZVN as precursors to make well-defined metallic nanostructures.

The reduction of NZVN to yield metallic nanostructures is a heterogeneous process that occurs at the reductant/NZVN interface and propagates through the solid. The electrons required for the reduction can be transported from solution (via a soluble chemical reducing agent),[6−12] gas phase (via a reducing gas such as H_2),[13] high-energy electron sources,[14] or

Received: July 18, 2011
Revised: September 29, 2011
Published: October 24, 2011

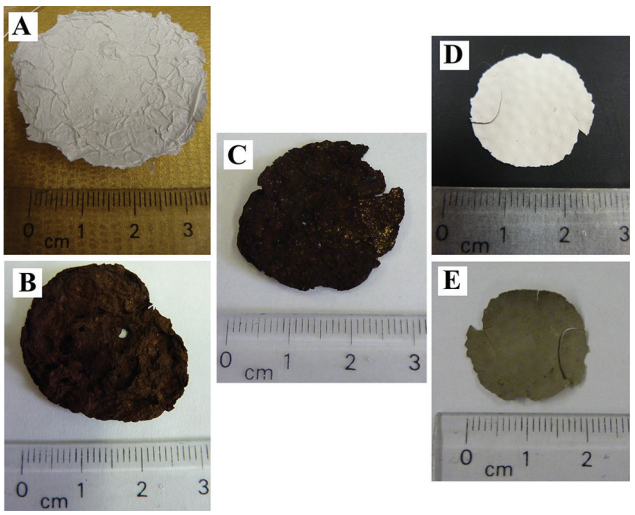

Figure 1. Photographs of the Au(I), Au(0), Ag(I), and Ag(0) nanostructured sheets. (A) AuCl(*n*-butylamine) sheet ($NS_{Au(I)}$). (B) Au(0) sheet made via reduction in toluene ($NS_{Au(0)\text{-}tol}$). (C) Au(0) sheet made via reduction in H_2O ($NS_{Au(0)\text{-}H2O}$). (D) AgCl sheet ($NS_{Ag(I)}$). (E) Ag(0) sheet ($NS_{Ag(0)}$).

from a solid. In the solid case, electrons can be provided by a substrate during photoreduction[15] (or thermolysis,[5,16−18]) or a solid electrode via electrochemical reduction.[19,20] Thermolysis is limited, however, by the low fusion temperature of metal nanostructures[21] and high-energy electron induced reduction is not applicable to large scale syntheses.

Electrochemical reduction has been used to produce small amounts of well-defined Ag(0) structures confined to the surface of a working electrode.[19,20] Our study of the chemical and electrochemical reduction of AgCN nanofiber networks to make a range of Ag(0) nanostructures (nanoprisms, nanoparticles, nanofibers) provides a starting point in understanding the processes operating in these systems.[10,19] Low reducing potentials generate Ag(0) structures whose geometries differ significantly from the parent anisotropic template, probably because of the partial dissolution of the AgCN template. Conversely, more reducing (cathodic) potentials preserve the initial fibrous geometry. This parallels observations that the use of a strong reducing agent such as $NaBH_4$ preserves the fibrous morphology of a silver oxalate fiber template, while a weaker reducing agent such as ascorbic acid produces a material with another morphology, likely involving the reduction of dissolved species rather than the reduction of the solid Ag(I) template.[9] The reduction of $TBA^+MBr_4^-$ vesicles (TBA^+: tetrabutylammonium, and M metal ion) with $NaBH_4$ preserves the original vesicle morphology. Similarly, with the electrochemical reduction of macroscopic AgCl electrodes, large overpotentials allow for a uniform reduction of the AgCl electrode, whereas lesser potentials generate nonuniformity.[22]

A general method for producing monolithic porous metals via the chemical reduction of solid assemblies of NZVN is presented here. The versatility of this technique is demonstrated by the conversion of large assemblies of Au(I) fibers and Ag(I) cubes into porous conductive monoliths composed of Au(0) fibers and Ag(0) cubes, respectively. The controlled aggregation of AuCl(*n*-butylamine) fibers and AgCl cubes leads to large sheets (cm^2) of Au(I) and Ag(I) nanostructures (Figure 1). These solid sheets can serve as sacrificial templates to yield monoliths of Au(0) and Ag(0) nanomaterials via chemical reduction (Figure 1). Complete reduction to the zerovalent state leads to the retention of the parent template morphology. The resulting multi-centimeter-square monoliths exhibit high electrical conductivity, suggesting that they will be excellent candidates for applications in catalysis and electrocatalysis.

EXPERIMENTAL SECTION

Materials and Methods. $HAuCl_4{\cdot}3H_2O$ (99.99%), AgCl (99.999%), and *n*-butylamine (99.5%) were obtained from Aldrich and used as received. The 2.5 cm wide membranes used to filter the AgCl cubes were made of polyvinylidene difluoride (PVDF), had a 0.45 μm pore size and were purchased from Millipore (catalogue #: HVLP 02500). The 4.7 cm membranes used to filter the AuCl(*n*-butylamine) fibers were made of polytetrafluoroethylene (PTFE), had a 0.45 μm pore size, and were purchased from Schleicher and Schuell (grade TE36).

Scanning electron microscopy (SEM) images were obtained using a FEG-SEM Hitachi S-4700 operated at 5 kV. Energy-dispersive X-ray spectroscopy (EDS) measurements were performed on the same FEG-SEM, using Oxford INCA EDS hardware. Typical conditions for spectral acquisition were as follows: size of the area analyzed: 5 μm; electron beam energy: between 6 and 10 kV; acquisition time: 90 s. Powder X-ray diffraction was performed using a Siemens D-5000 with a Globel mirror, using Cu Kα radiation. Samples were deposited on a glass slide. Thermogravimetric data were acquired under N_2 at a rate of 20 °C/min. Au/glass/Au slides were made via the evaporation of 5 nm of Ti, followed by 100 nm of Au, onto a glass slide (Fisher). A thin copper wire was used as a physical mask to make the junctions. The conductivity measurements were performed using a chi760c electrochemical workstation.

Synthesis of AuCl(THT).[23] $HAuCl_4{\cdot}3H_2O$ (1.469 g) was dissolved in 2.5 mL Milli-Q water and 12.5 mL ethanol. Tetrahydrothiophene (THT) (700 μL) was added dropwise to the stirring solution. A white precipitate immediately formed. The reaction was stirred 15 min before filtering. Small portions of ethanol (25 mL) were used to wash the precipitate. After vacuum drying overnight, we obtained 1.104 g of AuCl(THT). Yield: 92.3%.

Synthesis of $NS_{Au(I)}$: AuCl(*n*-butylamine) Nanofiber Sheet. AuCl(THT) (450 mg) was dissolved in 250 mL toluene in a 500 mL Erlenmyer flask. *N*-butylamine (170 μL) diluted in 4 mL of toluene was added dropwise to the stirring solution (400 rpm). A white precipitate quickly formed. The cloudy white solution was stirred for 5 min and was left to rest for 30 min. Filtration over a 4.7 cm PTFE membrane and drying in a vacuum oven produced a 4.5 cm circular soft sheet of white AuCl(*n*-butylamine) fibers. Yield: 83.3%

Synthesis of $NS_{Au(0)\text{-}tol}$: Au(0) Nanofoam. One circular sheet of ~350−375 mg of AuCl(*n*-butylamine) was dropped into 50 mL of toluene in a 150 mL beaker. Tetrabutylammonium borohydride ($[TBA][BH_4]$) (11 g) dissolved in 12 mL of a 3:1 ethanol/solution (forming a viscous clear solution) was added on the side of the beaker using a Pasteur pipet. A two-phase solution resulted. The toluene phase with the Au(I) sheet was at the bottom of the beaker, while the added solution of $[TBA][BH_4]$ was on top. Upon mixing with a Pasteur pipet, rapid reduction of the Au(I) sheet occurred, forming a purplish foamy precipitate which floated at the surface of the solution. The reaction mixture was left for 24 h (after 15 h, the solution was homogenized using a Pasteur pipet) after which the reddish foam was washed successively with copious amounts of ethanol and dichloromethane. A circular soft reddish foam resulted. Yield: 99.8%.

Synthesis of $NS_{Au(0)\text{-}H2O}$: Au(0) Nanofoam (see video S1). One circular sheet of ~350−375 mg of AuCl(*n*-butylamine) was dropped into a 200 mL beaker filled with 80 mL of a 1:1 methanol/Milli-Q water solution. A fresh aqueous solution of sodium borohydride (3.5 g of $NaBH_4$ dissolved in 45 mL Milli-Q water) was added on the side of the beaker using a Pasteur pipet. Rapid reduction of the Au(I) sheet occurred, producing a purplish foam which floated at the surface of the solution. The reaction mixture was left for 24 h (after 15 h, the solution was homogenized using a Pasteur

dx.doi.org/10.1021/cm2020498 | *Chem. Mater.* 2011, 23, 4954−4959

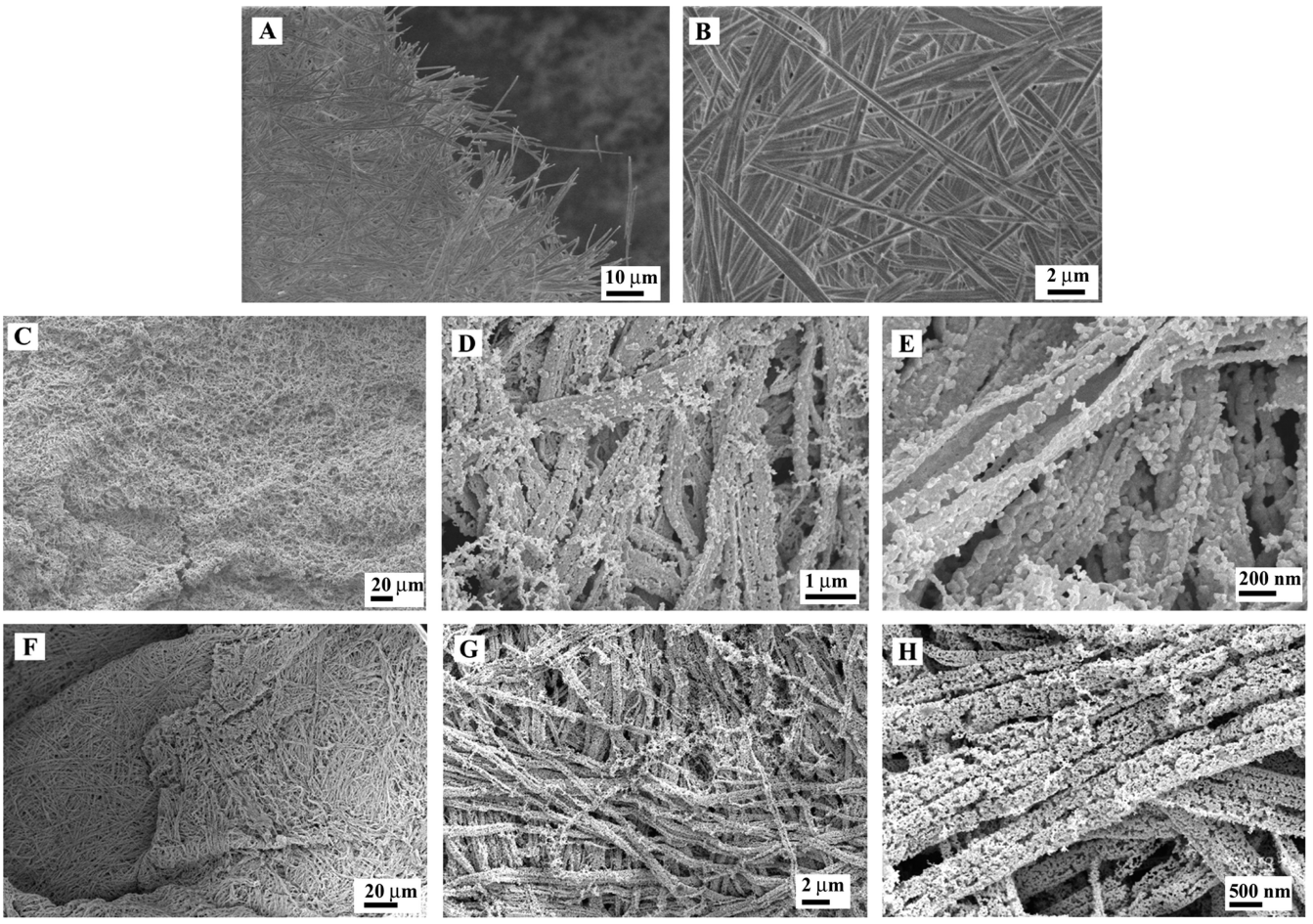

Figure 2. SEM images of the Au(I) and Au(0) structures produced. (A, B) $NS_{Au(I)}$. (C–E) $NS_{Au(0)\text{-}tol}$. (F–H) $NS_{Au(0)\text{-}H2O}$.

pipet) after which the purple foam was washed successively with a fresh sodium borohydride solution (350 mg $NaBH_4$ in 50 mL Milli-Q), followed by copious amounts of Milli-Q water, ethanol, and dichloromethane. A circular soft, reddish foam resulted. Yield: 99.7%.

Synthesis of $NS_{Ag(I)}$: AgCl nanocube sheet. AgCl (300 mg) was mixed with 15 mL cold dichloromethane and 3 mL of cold *n*-butylamine. Short ultrasonication (~1 min) was used to dissolve AgCl, forming a clear transparent solution. Dichloromethane and *n*-butylamine were stored in a freezer to avoid the reduction of Ag^+ to Ag(0) by the amine. The AgCl-butylamine-dichloromethane solution was added in one addition to a vigorously stirring (~700 rpm) 300 mL solution of acetone (500 mL Erlenmeyer flask). The flask was covered with aluminum foil to avoid photodecomposition of AgCl. The solution turned cloudy-white immediately due to AgCl precipitate formation. The solution was stirred for 1 min after the addition, and then filtered on a 2.5 cm PVDF membrane. Under our experimental conditions, the filtration took ca. 1 h. After drying under vacuum, a white solid circular sheet composed of pure silver chloride results. The dimensions of the AgCl sheet were similar to the membrane used (i.e., 2.5 cm). Yield: 74.3%.

Synthesis of $NS_{Ag(0)}$: Ag(0) porous sheet (see video S2). One circular sheet (~225 mg) of AgCl cubes was dropped into 50 mL of a 1:1 methanol:Milli-Q water solution. A fresh aqueous solution of sodium borohydride (2.2 g of $NaBH_4$ dissolved in 25 mL Milli-Q water) was added on the side of the beaker using a Pasteur pipet. The reduction was immediate and was seen as a rapid change in color of the white Ag(I) sheet to black. The reaction was left undisturbed for 24 h. Washing of the sheet (200 mL of Milli-Q water and 100 mL acetone) leads to a gray-silver circular sheet composed of aggregated Ag(0) porous cubes. Yield: 99.9%

RESULTS AND DISCUSSION

AuCl(*n*-butylamine) self-assembles in toluene to form very long nanofibers. Chaudret et al. previously reported the formation of AuCl(alkylamine) nanofibers with the reaction of long chain alkylamines (6 to 16 carbon chains) with AuCl, likely promoted by strong Au(I)–Au(I) interactions.[13] Thermolysis of these nanofibers, and their reduction with H_2, led to the formation of gold nanoparticles within the Au(I) fibers.[13] This work was followed by several reports where gold nanowires were synthesized from fibrous AuCl(oleylamine) precursors.[18] These reports motivated us to synthesize AuCl(*n*-butylamine), which to our knowledge, has not been previously reported. AuCl(THT) (THT = tetrahydrothiophene) served as a reactive Au(I) precursor to form the AuCl(*n*-butylamine) nanofibers (see Experimental Section).[14]

Reaction of AuCl(THT) with *n*-butylamine in toluene leads to a white precipitate. SEM establishes this to be composed of very long nanofibers (>20 μm in length, average diameter: 500 ± 200 nm, Figure S1 in the Supporting Information). Deposition of the AuCl(*n*-butylamine) complex from a toluene solution onto a polytetrafluoroethylene membrane (0.45 μm) produces a dense sheet of white AuCl(*n*-butylamine) nanofibers (named $NS_{Au(I)}$, Figure 1 and 2).These sheets are self-supporting, fairly flexible, and can be manipulated with tweezers without significant damage. Filtration on nanoporous membranes is a simple means to make free-standing films composed of various nanomaterials such as carbon nanotubes and cadmium hydroxide nanofibers.[24,25] Sheets of 350 mg of

dx.doi.org/10.1021/cm2020498 | *Chem. Mater.* 2011, 23, 4954–4959

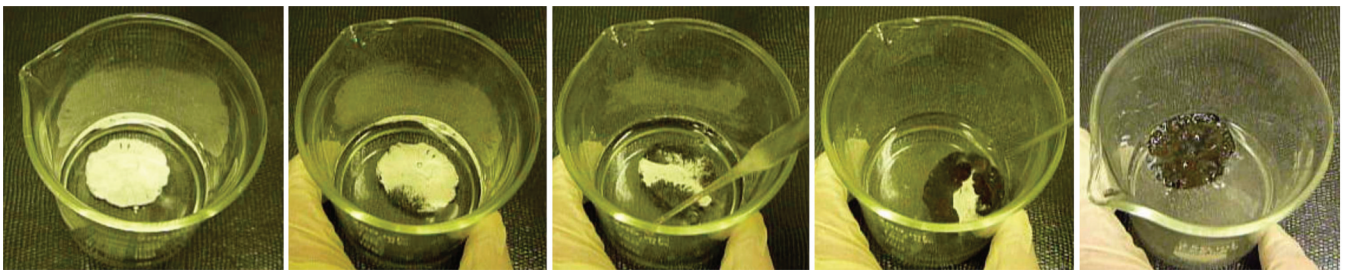

Figure 3. Photographs showing the time evolution of the reduction of $\mathbf{NS}_{\mathbf{Au(I)}}$ (left) to form $\mathbf{NS}_{\mathbf{Au(0)\text{-}tol}}$ (right). The propagation of the reduction boundary is clearly observable.

AuCl(*n*-butylamine) with areas exceeding 12 cm^2 (yield: 83.4%) were prepared. NMR and thermogravimetric analysis (TGA) studies confirm that these fibers are indeed composed of AuCl(*n*-butylamine) (see Figures S6 and S13 in the Supporting Information). Chemical reduction of the free-standing Au(I) sheets using [TBA][BH_4] in a toluene/ethanol solution (sample named $\mathbf{NS}_{\mathbf{Au(0)\text{-}tol}}$) or $NaBH_4$ in a Milli-Q water/methanol solution (sample named $\mathbf{NS}_{\mathbf{Au(0)\text{-}H2O}}$) (Figure 1 and 2) occurs at the solvent/Au(I) sheet interface. The propagation of the reduction boundary is clearly seen in reaction time series captured on video (Figure 3 and video S1 in the Supporting Information). The monolithic porous Au(0) is composed of interconnected 500 ± 230 nm wide ribbons (in the case of $\mathbf{NS}_{\mathbf{Au(0)\text{-}tol}}$, see Figure S2 in the Supporting Information) or 550 ± 150 nm wide fibers (in the case of $\mathbf{NS}_{\mathbf{Au(0)\text{-}H2O}}$, see Figure S3 in the Supporting Information). These Au(0) nanomaterials are distinctly different from the gold nanoparticles obtained by Chaudret et al.[13] and the gold nanowires synthesized by the groups of Xia, Lieber, and Yang.[18]

The morphology of the parent fibers is retained in the case of both Au samples (Figure 2). While there is little variation in the width of the fibers after reduction, $\mathbf{NS}_{\mathbf{Au(0)\text{-}tol}}$ is composed of Au(0) continuous nanoribbons, and $\mathbf{NS}_{\mathbf{Au(0)\text{-}H2O}}$ is composed of discontinuous nanofibers. The differences in the morphology of $\mathbf{NS}_{\mathbf{Au(0)\text{-}tol}}$ and $\mathbf{NS}_{\mathbf{Au(0)\text{-}H2O}}$ are attributed to the differences in swelling of the Au(I) polymer. In the water−methanol mixture, the fibers are completely insoluble and the material reduced under these conditions is expected to be very similar to the nanofibers observed in the solid state with SEM. On the other hand, in toluene, the nanofibers tend to form a gelatinous precipitate. We thus conclude that the Au(I) polymer conformation in toluene alters the Au(I) nanofiber geometry, leading to ribbonlike Au(0) structures. Porous sheets containing approximately 225 mg of Au(0) were synthesized (yield of the reduction reaction: 99.8%). Powder X-ray diffraction, TGA, infrared absorption, and energy dispersive analyses (EDS) confirm that it is entirely Au(0) (see Figures S6, S8−9, and S12 in the Supporting Information). A small amount of residual organic (~0.5%) was observed in $\mathbf{NS}_{\mathbf{Au(0)\text{-}H2O}}$ via TGA and EDS (see Figure S6 and S12 in the Supporting Information).

The generality of this method for producing metal foams was investigated with sheets formed from AgCl nanocubes. $CuCl_2{\cdot}2H_2O$ in dichloromethane dissolves in the presence of an excess of *n*-butylamine.[26] Similarly, an excess of *n*-butylamine dissolves AgCl in dichloromethane. Upon dilution in acetone, the AgCl-butylamine complex precipitates as AgCl cubes.[27] We were unable to isolate the AgCl-butylamine complex as removal of the dichloromethane from the AgCl-butylamine solution yields pure AgCl. Filtration of the AgCl cubes on a 2.5 cm polyvinylidene difluoride membrane (0.45 μm), followed by washings, produces a solid white sheet composed of aggregated AgCl cubes ($\mathbf{NS}_{\mathbf{Ag(I)}}$, Figures 1 and 4,

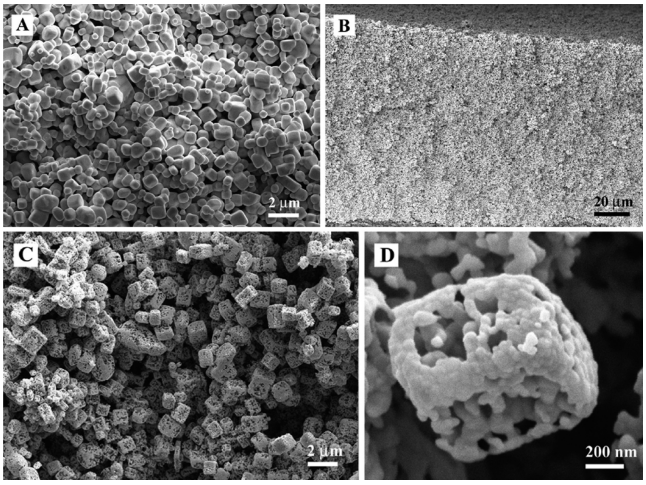

Figure 4. SEM images of the Ag(I) and the Ag(0) structures produced. (A) $\mathbf{NS}_{\mathbf{Ag(I)}}$. (B−D) $\mathbf{NS}_{\mathbf{Ag(0)}}$. B is a transverse cut of the Ag(0) sheet, showing that the sheet is made of connected porous Ag(0) cubes.

yield: 74.3%). The rapid recrystallization of silver halide microcrystals upon filtration, producing morphological changes, is a well-known phenomenon.[28] However, under the experimental conditions used here, the aggregation of the AgCl cubes is controlled and their original cubic morphology is maintained. A thin, hard white sheet composed of aggregated Ag(I) cubes (average side length: 650 ± 240 nm) forms upon deposition and drying on the filtration membrane (Figures 1 and 4, and Figure S4 in the Supporting Information). Reduction of $\mathbf{NS}_{\mathbf{Ag(I)}}$ with $NaBH_4$ in a 1:1 methanol:Milli-Q water solution generates a porous monolith composed of pure Ag(0) hollow cubes (sample named $\mathbf{NS}_{\mathbf{Ag(0)}}$), as verified by TGA, XRD, and EDS analyses (see Figures S7 and S10−12 in the Supporting Information).[29] The conversion of solid Ag(I) cubes into Ag(0) hollow cubes (average side length: 750 ± 250 nm, see Figure S5 in the Supporting Information) is attributed to a classical Kirkendall effect,[30] as per the reduction of Ag_3PO_4 microcrystals and Ag_2O nanoparticles in solution.[6,12] The increased porosity induced by the conversion of AgCl to Ag(0) is consistent with the large decrease in volume (47%) anticipated in this transformation. The fact that the cube retains its morphology and actually slightly increases in size (+100 nm on average) after the reduction supports this argument.

dx.doi.org/10.1021/cm2020498 | *Chem. Mater.* 2011, 23, 4954−4959

The chemical reduction of these large assemblies of NZVN is most likely a solid−solid conversion (Figure 3 and videos S1 and S2 in the Supporting Information). The clarity of the solutions in which the reactions occur, and the near quantitative yields of the M(I) to M(0) conversion, are consistent with a solid−solid conversion process. The Au(0) foams can be pressed onto Au/glass/Au junctions (glass width ca. 250 μm), acting as a cold solder. Two-point probe electrical conductivity measurements of these junctions demonstrated $\mathbf{NS}_{\mathbf{Au(0)\text{-}tol}}$ to be reasonably conductive (1820 S m^{-1}, see Figure S14 in the Supporting Information). Although 4 orders of magnitude lower than the conductivity of bulk gold ($\sigma_{Au} = 4.52 \times 10^7$ S m^{-1}),[31] the conductivity of $\mathbf{NS}_{\mathbf{Au(0)\text{-}tol}}$ is 3 orders of magnitude higher than the value reported for a high-surface-area, self-supported gold foam (i.e., 1.5 S m^{-1}).[2] The relatively high conductivity of these Au(0) foams is attributed to the synthetic pathway employed here: during the reduction process, the Au(0)/Au(I) boundary moves along the sheet, contributing to the formation of electrically connected metallic nanostructures. This solid−solid conversion leads to highly conductive nanomaterials, similar to the conductive Ag(0) nanostructures obtained *via* the electrochemical reduction of AgCN nanofibers.[19] BET measurements establish a surface area of 2 $m^2 g^{-1}$ or 400 m^2 mol^{-1} for $\mathbf{NS}_{\mathbf{Au(0)\text{-}tol}}$ (0.9 m^2 g^{-1} or 100 m^2 mol^{-1} for $\mathbf{NS}_{\mathbf{Ag(0)}}$), a value comparable to the highest surface area ever reported for monolithic gold nanofoams (10.9 m^2 g^{-1}).[2] Porous gold monoliths obtained via dealloying processes typically have BET-measured surface area values of ca. 1.5 m^2 g^{-1}.[32] Average pore widths from BET measurements are 9 nm for $\mathbf{NS}_{\mathbf{Au(0)\text{-}tol}}$ and 3 nm for $\mathbf{NS}_{\mathbf{Ag(0)}}$. Reliable measurements of the conductivity of the Ag(0) sheets could not be obtained because the Ag sheets are very brittle. The use of silver paste to improve the quality of the electrical contacts between the Ag(0) sheet and the electrodes was unsuccessful because of the capillary penetration of the silver paste into the porous sheet.

CONCLUSION

We have reported here the successful synthesis of cm^2-scale AuCl(*n*-butylamine) nanofiber and AgCl nanocube assemblies. These solid Au(I) and Ag(I) structures are converted into metal monoliths composed of Au(0) nanofibers and Ag(0) hollow nanocubes, respectively. These monoliths are both conductive and porous. The high-yield synthesis employed here is effective at room temperature and takes advantage of the aggregation of Au(I) fibers and Ag(I) cubes. It does not involve the elevated pressures or high temperature reactions that are required in combustion methods.[2] The total yields of this synthetic pathway (i.e., taking into account the yields of the reactions used to synthesize the Au(I) and Ag(I) nanostructure precursors) are 76.7% for Au and 74.3% for Ag. These are relatively high yields for the solution-phase synthesis of nanostructures. The approach presented here is general and should be applicable to a range of NZVN, leading to the production of a number of porous metallic foams.

ASSOCIATED CONTENT

Supporting Information

IV curves, videos, size distributions, powder XRD, EDS and NMR spectra, TGA data. This material is available free of charge via the Internet at http://pubs.acs.org

AUTHOR INFORMATION

Corresponding Author

*E-mail: bruce.lennox@mcgill.ca.

Author Contributions

The manuscript was written through contributions of all authors. All authors have given approval to the final version of the manuscript.

ACKNOWLEDGMENTS

The authors thank the Natural Sciences and Engineering Research Council of Canada and the Centre for Self-Assembled Chemical Structures for their financial support.

REFERENCES

(1) Lou, X. W.; Archer, L. A.; Yang, Z. *Adv. Mater.* **2008**, *20*, 3987−4019.
(2) Tappan, B. C.; Steiner, S. A. III; Luther, E. P. *Angew. Chem., Int. Ed.* **2010**, *49*, 4544−4565.
(3) Gurney, R. W.; Mott, N. F. *Proc. R. Soc., Ser. A* **1938**, *164*, 151−167.
(4) James, T. H.; Kornfeld, G. *Chem. Rev.* **1942**, *30*, 1−32.
(5) Corbierre, M. K.; Beerens, J.; Lennox, R. B. *Chem. Mater.* **2005**, *17*, 5774−5779.
(6) Yang, J.; Qi, L.; Lu, C.; Ma, J.; Cheng, H. *Angew. Chem., Int. Ed.* **2005**, *44*, 598−603.
(7) Zhang, X.; Li, D. *Angew. Chem., Int. Ed.* **2006**, *45*, 5971−5974.
(8) Su, X.; Zhao, J.; Bala, H.; Zhu, Y.; Gao, Ye; Ma, S.; Wang, Z. *J. Phys. Chem. C* **2007**, *111*, 14689−14693.
(9) Wang, H.; Qi, L. *Adv. Funct. Mater* **2008**, *18*, 1249−1256.
(10) Lazzara, T. D.; Bourret, G. R.; Lennox, R. B.; van de Ven, T. G. M. *Chem. Mater.* **2009**, *21*, 2020−2026.
(11) Li, L.; Wang, Z.; Huang, T.; Xie, J.; Qi, L. *Langmuir* **2010**, *26*, 12330−12335.
(12) Ben Moshe, A.; Markovich, G. *Chem. Mater.* **2011**, *23*, 1239−1245.
(13) Gomez, S.; Philippot, K.; Colliere, V.; Chaudret, B.; Senocq, F.; Lecante, P. *Chem. Commun.* **2000**, 1945−1946.
(14) Halder, A.; Ravishankar, N. *J. Phys. Chem. B* **2006**, *110*, 6595−6600.
(15) Nishijo, J.; Oishi, O.; Judai, K.; Nishi, N. *Chem. Mater.* **2007**, *19*, 4627−4629.
(16) Wang, Z. L.; Kong, X. Y.; Wen, X.; Yang, S. *J. Phys. Chem. B* **2003**, *107*, 8275−8280.
(17) Judai, K.; Nishijo, J.; Nishi, N. *Adv. Mater.* **2006**, *18*, 2842−2846.
(18) (a) Lu, X.; Yavuz, M. S.; Tuan, H.-Y.; Korgel, B. A.; Xia, Y. *J. Am. Chem. Soc.* **2008**, *130*, 8900−8901. (b) Wang, C.; Hu, Y.; Lieber, C. M.; Sun, S. *J. Am. Chem. Soc.* **2008**, *130*, 8902−8903. (c) Huo, Z.; Tsung, C.-K.; Huang, W.; Zhang, X.; Yang, P. *Nano Lett.* **2008**, *8*, 2041−2044.
(19) Bourret, G. R.; Lennox, R. B. *ACS Appl. Mater. Interfaces* **2010**, *2*, 3745−3758.
(20) Bourret, G. R.; Lennox, R. B. *Nanoscale* **2011**, *3*, 1838−1844.
(21) Buffat, P.; Borel, J.-P. *Phys. Rev. A* **1976**, *13*, 2287−2298.
(22) Xiao, W.; Jin, X.; Deng, Y.; Wang, D.; Chen, G. Z. *Chem.—Eur. J.* **2007**, *13*, 604−612.
(23) Corbierre, M. K.; Lennox, R. B. *Chem. Mater.* **2005**, *17*, 5691−5696.
(24) Peng, X.; Jin, J.; Ericsson, E. M.; Ichinose, I. *J. Am. Chem. Soc.* **2007**, *129*, 8625−8633.
(25) Wu, Z.; Chen, Z.; Du, X.; Logan, J. M.; Sippel, J.; Nikolou, M.; Kamaras, K.; Reynolds, J. R.; Tanner, D. B.; Hebard, A. F.; et al. *Science* **2004**, *305*, 1273.
(26) Bourret, G. R.; Lennox, R. B. *J. Am. Chem. Soc.* **2010**, *132*, 6657−6659.
(27) Reaction between *n*-butylamine and acetone occurs. However, we observed that silver chloride also precipitates when the same

solution is diluted in dichloromethane. Since dichloromethane does not react with *n*-butylamine, we conclude that the complex becomes unstable when the concentration of *n*-butylamine is low (in either solvent), forming AgCl. The AgCl structures formed in dichloromethane were not as homogenous as the one produced in acetone.
(a) Carey, F. A. *Organic Chemistry*, 3rd ed.; McGraw-Hill: New York, 1996; p 700.
(28) Sugimoto, T.; Yamaguchi. *J. Cryst. Growth* **1976**, *34*, 253–262.
(29) The presence of a silver oxide layer was not detected by these measurements, but cannot be ruled out.
(30) Schröder, H.; Samwer, K.; Köster, U. *Phys. Rev. Lett.* **1985**, *54*, 197–200.
(31) Lide, D. R., *CRC Handbook of Chemistry and Physics*, 90th ed.; CRC Press: Boca Raton, FL, 2010.
(32) Nyce, G. W.; Hayes, J. R.; Hamza, A. V.; Satcher, J. H. Jr. *Chem. Mater.* **2007**, *19*, 344–346.